CrossMark

ORIGINAL PAPER

Behavior of compacted expansive soil under multi-directional stress and deformation boundary conditions

Tamer Y. Elkady[1,2] · Mohamed F. Abbas[1] · Mosleh A. Shamrani[1]

Abstract This study aims at investigating the effect of multi-direction stress and deformation boundary conditions on the volume change behavior of highly expansive compacted soils. Stress boundary condition refers to the stresses applied on the axial and lateral boundaries of the specimen. Deformation boundary condition refers to restraint imposed on the axial or lateral boundaries of the specimen. To this end, a series of response-to-wetting triaxial tests were carried out to simulate three boundary conditions; namely, constant isotropic stress (CIP), constant axial (CA) deformation, and constant volume (CV). In addition, a series of one-dimensional consolidation tests (oedometer tests) was performed to provide baseline information on volume change of expansive specimens under fully laterally restrained conditions. All tests, including the triaxial, axial stress and oedometer tests, were performed under a wide range of confining pressures, ranging between 50 and 800 kPa. Test results revealed that stress conditions had a significant effect on the magnitude and sign of strain realized during inundation of CIP and CA specimens. It was observed that axial restraint (in CA tests) or full restraint (in CV tests) induced time-dependent changes in stresses. In addition, this study demonstrated the effect of stress ratio, K, on the axial and volumetric swelling behavior of tested specimens. Finally, comparisons between triaxial and oedometer test results were conducted for realistic estimation of swelling strain under given boundary and stress conditions.

Keywords Expansive soils · Response-to-wetting · Stress ratio · Stress path · One-dimensional · Triaxial

Introduction

Extensive areas throughout the world, mainly in arid and semi-arid regions, experience foundation problems caused by expansive soils (Radevsky 2001; Houston et al. 2011; Dafalla and Shamrani 2011, 2012). Expansive soils undergo significant volume change with change in water content. There are two main parameters that are used to evaluate the characteristics of expansive soils: swelling pressure and swelling strain [as per the American Society for Testing and Materials (ASTM) standard D4546]. These swelling characteristics are important for the design of several structures such as pavements, shallow foundations, shallow tunnels, retaining walls, canal linings and underground conduits. So far, one-dimensional oedometer testing has been widely used to evaluate these parameters where a specimen is laterally restrained with volume change occurring in one direction only (i.e., the vertical direction). Oedometer testing of expansive soils is conducted by constant stress and constant volume testing (ASTM D4546). For a constant stress test, the specimen is allowed to swell in the vertical direction under constant applied vertical stress. For a constant volume test, a specimen's deformation is restrained in the vertical and lateral directions to determine swelling pressure. In "real life" engineering situations, swelling characteristics obtained from an oedometer is different than that recorded in the

✉ Tamer Y. Elkady
  tyelkady@yahoo.com

1 Department of Civil Engineering, College of Engineering, Bugshan Research Chair in Expansive Soils, King Saud University, P.O. 800, Riyadh 11421, Kingdom of Saudi Arabia

2 Soil Mechanics and Foundations Research Laboratory, Faculty of Engineering, Cairo University, Giza 12316, Egypt

field. Factors contributing to this difference were summarized by El-Sayed and Rabbaa (1986) and included stress path (Komornik and David 1969), state of stresses, scale effects (Sing 1967; Chen 1975; Ranganatham and Satyanarayana 1965; Rabbaa 1975), boundary conditions (Kassif and Baker 1969), sample disturbance (Ofer et al. 1983), and degree of wetting (Dhowian 1990; Wray et al. 2005). In regard to boundary conditions and state of stresses, expansive soils in the field are not considered fully restrained in the lateral direction as simulated using the laboratory oedometer. Therefore, in situ behavior of expansive soil may involve swelling in a vertical as well as lateral direction. Previous research reported that the ratio of one-dimensional swelling as per oedometer tests to vertical swelling observed in the field was about three (Gizienski and Lee 1965; Erol et al. 1987; Dhowian 1990). In other words, the vertical swelling realized in the field represents about one-third of the volume change indicated by the oedometer.

Bearing the above in mind, several researchers have been motivated to investigate the swelling characteristics of expansive soils under various boundary conditions and stress states. Recently, Tang et al. (2013) and Lui et al. (2014) suggested that there are infinite possible boundary conditions besides constant volume and constant stress conditions under which specimens may undergo swelling. They devised a modified oedometer to investigate the swelling characteristics under various constant stiffness conditions in addition to constant stress and constant volume conditions. Constant stiffness imposes a boundary condition of increasing vertical stress with an increase in swelling strain. They concluded that the swelling characteristics of tested specimens significantly depended on boundary conditions applied with the swelling pressure evaluated under constant stiffness lying between constant stress and constant volume conditions. On the other hand, several researchers investigated the effect of stress state on the swelling behavior of expansive soils using a triaxial device under isotropic and anisotropic stress conditions (Dakshanamurthy 1979; Tisot and Aboushook 1983; Al-Shamrani and Al-Mhaidib 1995, 1999; Al-Shamrani and Dhowian 2003; Chen and Ng 2005). It was reported that the volumetric strain of expansive soils depends on the mean stress applied on specimens (Dakshanamurthy 1979; Tisot and Aboushook 1983). It was also noted that the there is a significant difference between the swelling pressure deduced from oedometer tests and that deduced from triaxial tests under isotropic conditions (Tang et al. 2013). Tests conducted on expansive soils during wetting using a suction-controlled triaxial device revealed that the variation of volumetric strain with suction showed a non-linear relationship (Chen and Ng 2005).

Most of the previous research on expansive soils focused on the evaluation of vertical and/or volumetric swell strain with little attention given to stresses developed in specimens during swelling. Furthermore, the volume change behavior of expansive clay under stresses greater than swelling pressures have been rarely discussed. In this study, a series of response-to-wetting triaxial tests were performed to evaluate the multi-directional (lateral and axial) stress and strain behavior of compacted, expansive clay under different boundary conditions. Boundary conditions simulated included: constant isotropic pressure (CIP), constant axial (CA) deformations and constant volume (CV). Strains and/or stresses evolved during specimen inundation were recorded. Moreover, a comparison between volume change behavior of expansive clay under triaxial and oedometer conditions was performed. Finally, the effect of the ratio of lateral stress (σ_L) to axial stress (σ_a; i.e., stress ratio, K) on the volume change behavior of tested expansive soils was investigated.

Soil used

Geological setting

The expansive clay used in this study was obtained from the city of Al-Qatif located in the eastern province of Saudi Arabia (latitude 26°56′N and longitude 50°01′E) along the shoreline of the Arabian Gulf coastal region (Fig. 1). This clay is part of sedimentary strata present in the Arabian Gulf which range in age from the Jurassic to the Eocene eras. These sedimentary strata dip toward the east and northeast at a mild slope of 1 m/km until they merge with the Arabian Gulf (Slater 1983). The geology in the eastern part of the Arabian Peninsula comprises argillaceous shale and calcareous sedimentary rocks such as dolomite, limestone, marl and chert from the Permian, Cretaceous, and Tertiary eras (Saint-Marc 1978). The expansive clays of the Al-Qatif region are derived from these geological materials by the actions of geological and weathering processes. Geological processes included deformational processes like glacial activity and successive transgression and regression cycles of gulf seawater that occurred during the late Pleistocene and Holocene ages (Al-Sayari and Zotl 1978; El-Naggar 1988). Subsequent physical and chemical weathering combined with favorable climatic and environmental conditions of the Arabian Gulf region have facilitated the evolution of the expansive clay minerals in Al-Qatif clay. Favorable environmental conditions include flat topography, an alkaline environment, hot and arid climates, an abundance of clay-forming ions (Na^+, Ca^{2+}, Mg^{2+}, SO_4^{2+}) in pore water of sediment materials (Mitchell 1993), and inhibited leaching due to restrained mobility of highly alkaline water (Azam and Al-Shayea 1999).

Fig. 1 General layout of sampling area
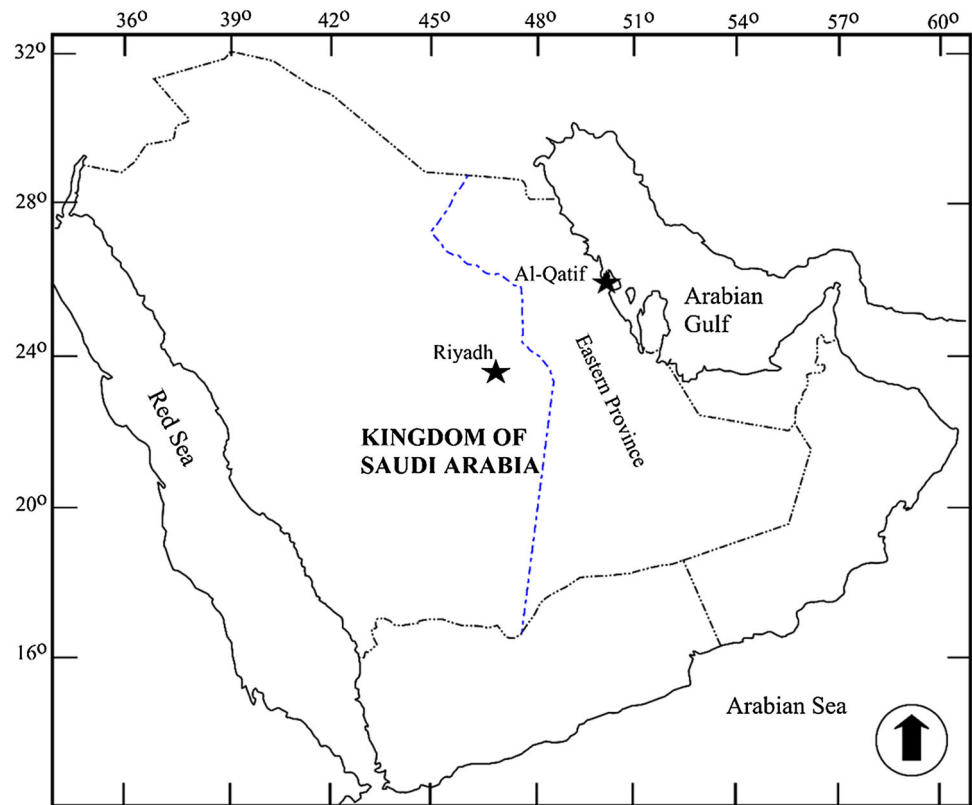
Soil sampling and characterization

Expansive clay samples were obtained from a test pit excavated to a depth of about 5.0 m below ground surface. The subsurface soil profile encountered during excavation is illustrated in Fig. 2. The expansive clay encountered at the site was classified as greenish gray, extremely fissured, highly overconsolidated clay, as shown in Fig. 3. Bulk soil samples were transported to the laboratory to perform routine geotechnical, physical, and mineralogical characterization. All geotechnical testing was conducted in accordance with ASTM test standards and using distilled water. Distilled water was produced using a water still device (model WSB/4, Hamilton Laboratory Glass, UK) . The liquid, plastic and shrinkage limits were 140, 60, and 20 %, respectively. The particle density of soil solids was 2.71 g/cm^3. The grain size distribution of test soil constitutes 38 % silt-size particles (0.075–0.002 mm) and 56 % clay-size particles (<0.002 mm), as shown in Fig. 4. The soil is classified as CH according to the Unified Soil Classification System (USCS). The aforementioned characterization data were consistent with the results of previous studies conducted on the same clay (Abduljuawad et al. 1992; Azam et al. 1998; Al-Shayea 2001; Azam 2003).

The mineralogical investigation of Al-Qatif soil conducted using X-ray diffraction (XRD) analysis revealed

Fig. 2 Subsurface profile at test pit sampling location—Al-Qatif, Kingdom of Saudi Arabia (KSA)

that the predominant clay minerals are montmorillonite and palygorsite which are typical expansive minerals. Quantitative analysis of Al-Qatif clay carried out by Abduljuawad (1994) revealed that the montmorillonite mineral constitutes about 52 % of its mineral composition.

Fig. 3 Photo documentation of sample obtained from sampling location

Specimen preparation

To ensure repeatability and minimize variability in test data due to soil heterogeneity, compacted clay specimens were used in this study. Bulk clay samples were air dried, pulverized, and sieved using sieve no. 40 (mesh opening size of 0.420 mm) to remove oversized particles and to obtain clay powder. The soil was hand mixed with distilled water at a target water content. Mixing was conducted for about 30 min to ensure uniform distribution of water in the mixture. To ensure moisture homogenization, the mixture was placed in hermetic plastic bags and stored in a humid environment for not less than 24 h. Tested specimens were statically compacted to final dimensions at maximum dry density (γ_d = 12 kN/m^3) and optimum moisture content (w_{op} = 32 %) evaluated using standard compaction effort as per ASTM D698.

Specimen dimensions for oedometer testing were 20 mm high and 50 mm in diameter. Triaxial tests specimens were 30 mm high and 75 mm in diameter
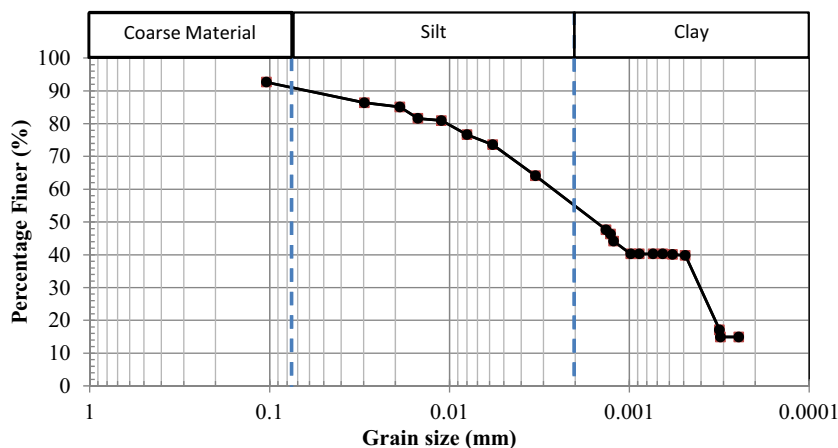
maintaining a height-to-diameter ratio similar to oedometer test specimens. It is worth noting that a specimen size smaller than that recommended in triaxial testing standards (i.e., height-to-diameter ratio = 2.0–2.5 as per ASTM D4767) was selected to reduce testing time. The specimen size recommended in triaxial standards was set to minimize the effect of friction between test specimens and triaxial platens (aka. end-platen friction) on shear strength. In this study, where the volume change behavior is of main interest, the end-platen friction effect is considered to have a minor effect. A discussion on the effect of end-platen friction on test results is provided later in this paper.

Equipment and test procedure

Triaxial tests

Triaxial testing was performed using a single-cell, computer-controlled stress path triaxial apparatus manufactured by GDS, UK. A schematic diagram showing the main components of the triaxial apparatus used in this study is shown in Fig. 5. The apparatus was equipped with two pressure volume controllers (PVCs) for the independent control of cell and back pressures. Specimen volume change was evaluated by noting the change in cell water volume recorded using cell PVCs. Axial loading and axial deformation were measured using a submersible load cell and external displacement transducer, respectively.

The general procedure for triaxial testing comprised three stages. In the first stage, compacted specimens were subjected to an isotropic confining pressure ($\sigma_c = \sigma_a = \sigma_L$; Fig. 6) and maintained until no volume change was recorded (typically for 30–60 min). Isotropic confining pressures (σ_c) considered were 50, 100, 200, 400, 600 and 800 kPa. In the second stage, specimens were inundated by admitting distilled water through the top drainage port under a nominal backpressure of 10 kPa with the bottom

Fig. 4 Grain size distribution of Al-Qatif clay
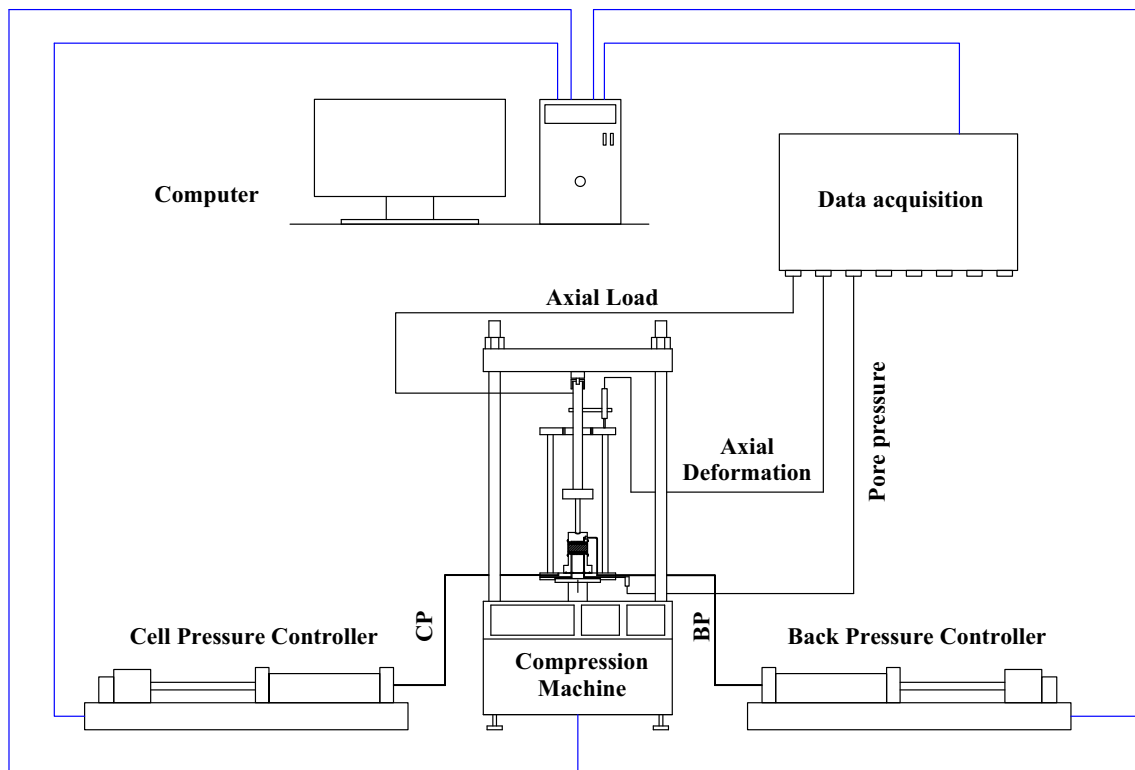
Fig. 5 Schematic diagram of the triaxial system used in this study

drainage port initially opened to allow the egress of air, which was then closed. The inundation process was maintained for 2–3 days to ensure full saturation of specimens and continued until equilibrium was attained (i.e., no change in specimen volume was recorded). Furthermore, back calculation of the degree of specimen saturation at the end of inundation revealed that the degree of saturation ranged between 96 and 100 %. The third stage constituted specimen unloading after attaining the final volume change. During the second stage, three test series were performed simulating volume change under different boundary and stress conditions as detailed below. A schematic diagram of test boundary and stress conditions before and at the end of inundation are provided in Fig. 6.
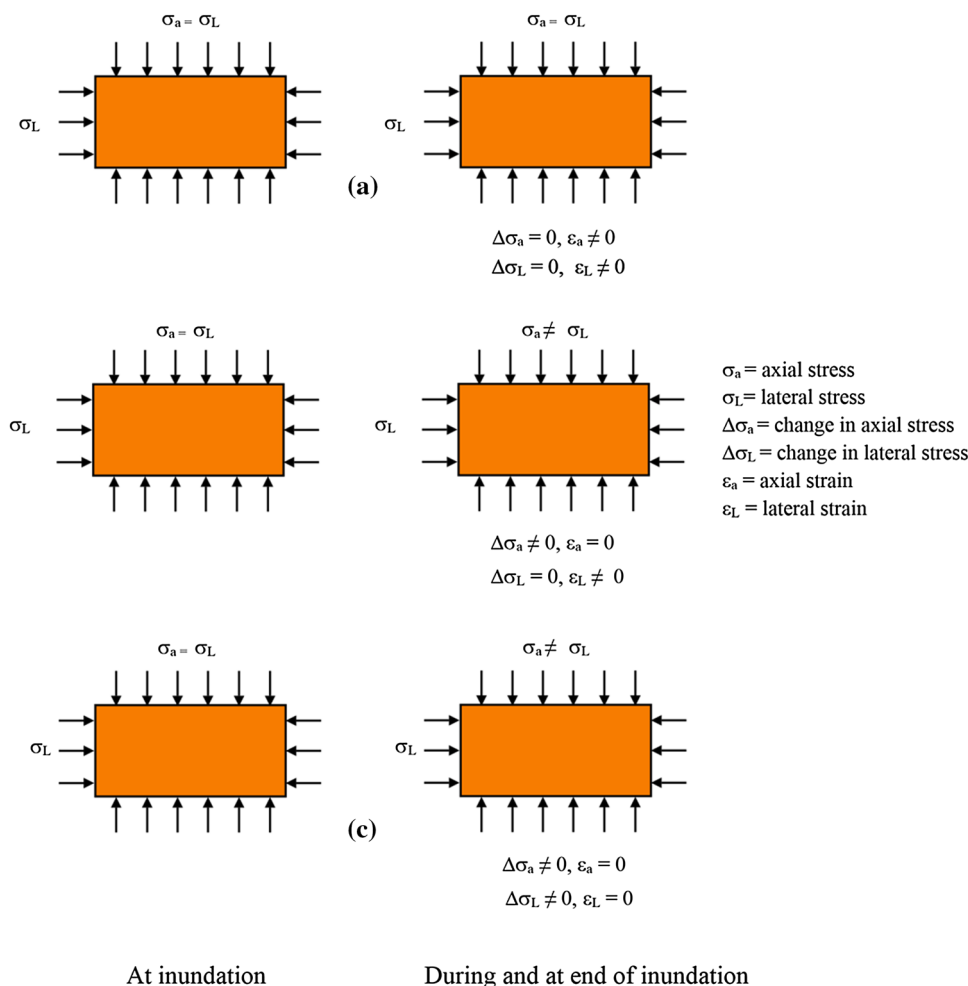
- *Constant isotropic pressure (CIP) test* specimens were inundated under a constant isotropic confining pressure (σ_c) applied during the first stage. During inundation, the confining pressure remained constant and axial and volumetric strains developed were recorded (Fig. 6a).
- *Constant axial (CA) deformation tests* specimens were inundated with a full restrained boundary in the axial direction and a free deformation boundary condition in the lateral direction (Fig. 6b). This condition was simulated by fixing the movement of axial loading ram while maintaining lateral stress (σ_L) constant. Under this condition, specimens were permitted to

swell in the lateral direction only. Lateral swell strain developed was recorded using cell PVCs. Deviator stress $q = (\sigma_a - \sigma_L)$ generated during inundation was recorded using the load cell.
- *Constant volume (CV) tests* In this test series, swelling of test specimens was restrained in both the axial and lateral directions by restraining the movement of the axial loading ram and cell PVC ram (Fig. 6c). Axial and lateral swell stresses were evaluated from the increase in deviator stress and cell pressure, respectively. It should be noted that specimens were not considered fully restrained in the lateral direction due to the compressibility of water, the flexibility of the plastic tubes connecting PVCs to the cell, and the cell volume change. Nevertheless, the maximum error in lateral strain measured was in order of 1.3 % (discussed later) which was deemed insignificant.

In addition to the above, a series of swell triaxial tests were conducted to investigate the effect of anisotropic stress conditions (i.e., $\sigma_a \neq \sigma_L$) on the volume change behavior of expansive soils. In this test series (referred to herein as CAP), the stress and boundary conditions are similar to CIP tests with the exception that the specimen at inundation was subjected to an axial stress of 50 kPa with varying stress ratios ($K = \sigma_L/\sigma_a$) of 0.5 and 1.5. A summary of all triaxial test conditions are presented in Table 1.

Fig. 6 Stress and boundary
condition **a** CIP, **b** CA and **c** CV
specimens

$\sigma_a = \sigma_L$

σ_L

$\sigma_a = \sigma_L$

σ_L

(a)

$\Delta\sigma_a = 0, \varepsilon_a \neq 0$
$\Delta\sigma_L = 0, \varepsilon_L \neq 0$

$\sigma_a = \sigma_L$

σ_L

$\sigma_a \neq \sigma_L$

σ_L

σ_a = axial stress
σ_L = lateral stress
$\Delta\sigma_a$ = change in axial stress
$\Delta\sigma_L$ = change in lateral stress
ε_a = axial strain
ε_L = lateral strain

$\Delta\sigma_a \neq 0, \varepsilon_a = 0$
$\Delta\sigma_L = 0, \varepsilon_L \neq 0$

$\sigma_a = \sigma_L$

σ_L

$\sigma_a \neq \sigma_L$

σ_L

(c)

$\Delta\sigma_a \neq 0, \varepsilon_a = 0$
$\Delta\sigma_L \neq 0, \varepsilon_L = 0$

At inundation   During and at end of inundation

Triaxial calibrations

The cell PVCs were used to measure volume change of test
specimens based on cell water ingress or egress with a
transducer accuracy of 1.0 mm^3. However, there are a
number of factors that may affect the overall accuracy of
the PVC volume change measurement. Error in PVC vol-
ume measurements (also referred to as apparent volume
change) are attributed to: (1) immediate volume change
due to the expansion/contraction of the cell wall, con-
necting tubes and cell water caused by the change in cell
pressure; and (2) temperature-dependent volume change
(Ng et al. 2002). To quantify the apparent volume change
(AVC) for each error, a series of calibrations were per-
formed. During calibrations, a stainless steel dummy
specimen was used between the load platens of the triaxial
apparatus to eliminate specimen volume changes. The first
calibration involved increasing cell pressure up to the
maximum value expected during testing (800 kPa) fol-
lowed by unloading. For each cell pressure increment or
decrement, the target pressure was ramped up within 2 min

and the AVC was recorded using PVCs. The variation of
AVC with applied pressure showed a linear relationship, as
shown in Fig. 7. Moreover, conducting the calibration for
two cycles showed that the data is repeatable with slight
differences between the loading and unloading paths. This
relationship was used to adjust volume change measure-
ments recorded during the test.

To evaluate the temperature-dependent AVC, a second
series of tests was performed in which cell pressure was
applied and maintained for about 1 week. During this
period, AVC and "on-cell" temperature were recorded.
On-cell temperatures were recorded using a thermocouple
sensor attached to the triaxial cell. Variation of "on cell"
temperature and AVC with time is shown in Fig. 8. From
Fig. 8, it is observed that the on-cell temperature and AVC
vary in tandem with an 80-min response delay between
AVC and on-cell temperature (see insert in Fig. 8). From
this data, the error in PVC volume due to temperature was
estimated to be in the order of 345 mm^3/°C which is
equivalent to volumetric strain of 0.22 %/°C for a speci-
men size 30 mm high and 75 mm in diameter.

Table 1 Summary of triaxial tests conditions and results

Specimen ID	K	σa (kPa)	Strains (%)			Stresses (kPa)			
			Axial	Lateral	Volumetric	Axial swelling stress		Lateral swelling stress	
			εa	εL	εv	Peak	Residual	Peak	Residual
CIP_50[a]	1.0	50	10.90	3.69	18.29	–	–	–	–
CIP_100	1.0	100	6.81	1.45	9.71	–	–	–	–
CIP_250	1.0	250	2.58	−0.30	1.98	–	–	–	–
CIP_400	1.0	400	1.17	−1.11	−1.04	–	–	–	–
CIP_600	1.0	600	−1.86	−2.36	−4.73	–	–	–	–
CIP_800	1.0	800	−1.43	−3.00	−4.09	–	–	–	–
CA_50	1.0	55	–	4.92	9.84	220	148	–	–
CA_100	1.0	100	–	2.55	5.10	211	172	–	–
CA_250	1.0	250	–	1.19	2.38	310	283	–	–
CA_400	1.0	400	–	−0.8	−1.7	466	423	–	–
CA_600	1.0	600	–	−1.71	−3.42	548	549	–	–
CA_800	1.0	800	–	−2.31	−4.6	700	720	–	–
CV_50	1.0	50	–	0.91	1.82	271	240	186	183
CV_50	1.0	50	–	0.78	1.55	284	247	195	164
CV_150	1.0	150	–	0.47	0.93	333	287	240	215
CV_250	1.0	250	–	0.26	0.51	330	299	317	288
CV_400	1.0	400	–	−0.42	−0.85	343	347	332	338
CV_600	1.0	600	–	−1.27	−2.53	454	467	414	414
CV_800	1.0	800	–	−1.15	−2.30	627	643	619	633
CAP_0.5	0.5	25	6.5	2.80	12.00	–	–	–	–
CAP_1.5*	1.5	75	13.7	2.90	19.50	–	–	–	–

[a] Replicate tests were conducted as shown in Figs. 18, 19 and 20

Fig. 7 Variation of immediate AVC with cell pressure

$y = 0.018x + 0.352$
$R^2 = 0.998$
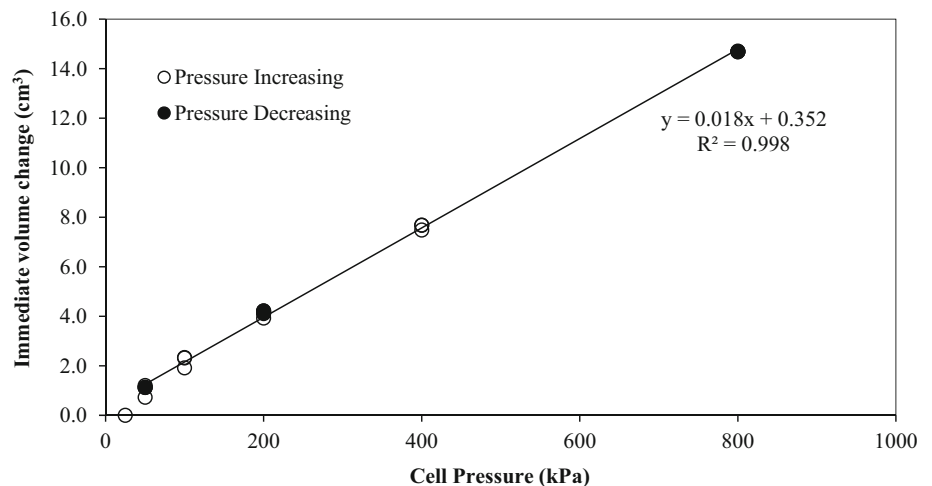
Oedometer testing

For the sake of comparison, a series of response-to-wetting tests using an oedometer was performed to evaluate the volume change behavior (whether swell or collapse) of tested specimens under lateral restraint conditions. Tests performed were in accordance with ASTM D4546 and included: (1) inundation under constant stress test (ASTM D4546—Method B) and (2) constant volume test (ASTM D4546—Method C). For method B tests, specimens were inundated under varying axial stresses of 50, 100, 200, 400, 600, and 800 kPa. All specimens were inundated using distilled water. For the convenience of reference, in the remainder of this paper, method B oedometer tests are

Fig. 8 Variation of AVC and on-cell temperature with elapsed time
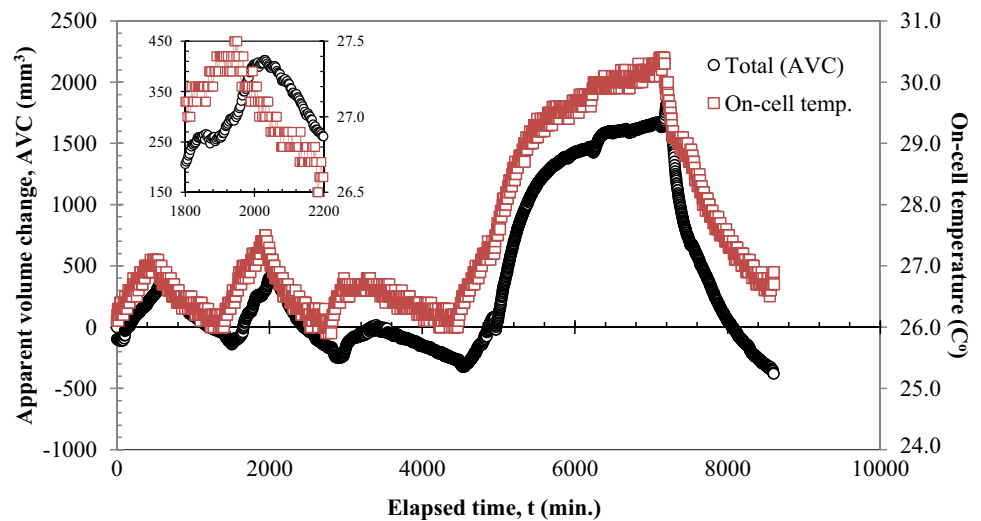
Table 2 Summary of the conditions and the results for oedometer testing program

Specimen ID	K	σv (kPa)	Strain (%)		Swelling pressure (kPa)
			Axial	Volumetric	
O_B_50[a]	Ko	50	16.81	16.81	470
O_B_100	Ko	100	7.23	7.23	400
O_B_200	Ko	200	3.69	3.69	415
O_B_300	Ko	300	0.34	0.34	320
O_B_400	Ko	400	−0.98	−0.98	–
O_B_600	Ko	600	−4.37	−4.37	–
O_B_800	Ko	800	−5.46	−5.46	–
O_C_50	Ko	50	–	–	300

[a] Replicate tests were conducted as shown in Figs. 13 and 15

labeled (O_B_Vt) where Vt symbolizes the vertical stress under which test specimens are inundated. The constant volume test is labeled (O_C). A summary of oedometer test conditions considered in this study is presented in Table 2.

Results and discussion

This section summarizes the results of the experimental program described earlier. The effect of boundary conditions on the response to swelling was evaluated with respect to multi-directional (i.e., axial, lateral and volumetric) strains and stresses. Furthermore, the effect of stress ratio, K, on volume change behavior of the tested soil was discussed.

Response-to-wetting curves

The aim of this section is to illustrate the different trends of response-to-wetting curves (stress–strain curves) observed as a result of inundation of swelling specimens under

different boundary conditions considered in this study. These response-to-wetting curves are used to graphically portray the change in stress and strain for triaxial specimens as a result of dry loading, inundation, and unloading. Response-to-wetting curves for triaxial specimens shown in Figs. 9, 12 and 13 illustrate the variation of strain with the logarithm of stress. On the other hand, stress–strain curves for O_B and O_C specimens are illustrated in Figs. 10 and 11 respectively. For the sake of clarity, only selected data sets were presented.

Response-to-wetting curves for CIP specimens under different applied stresses are illustrated in Fig. 9. Figure 9a depicts the relationship between the logarithm of axial stress (σ_a) and axial strain (ε_a), while Fig. 9b illustrates the relationship between logarithm of mean stress (p) and volumetric strain (ε_v). The mean stress (p) is calculated as ($\sigma_a + 2\sigma_L$)/3. Because axial and lateral stresses remain constant during inundation of CIP specimens, the volume change behavior (whether swell or collapse) is represented by a vertical line on the σ_a–ε_a or p–ε_v plots (e.g., line 1–1′ on Fig. 9).

Fig. 9 Response-to-wetting curves for CIP specimens
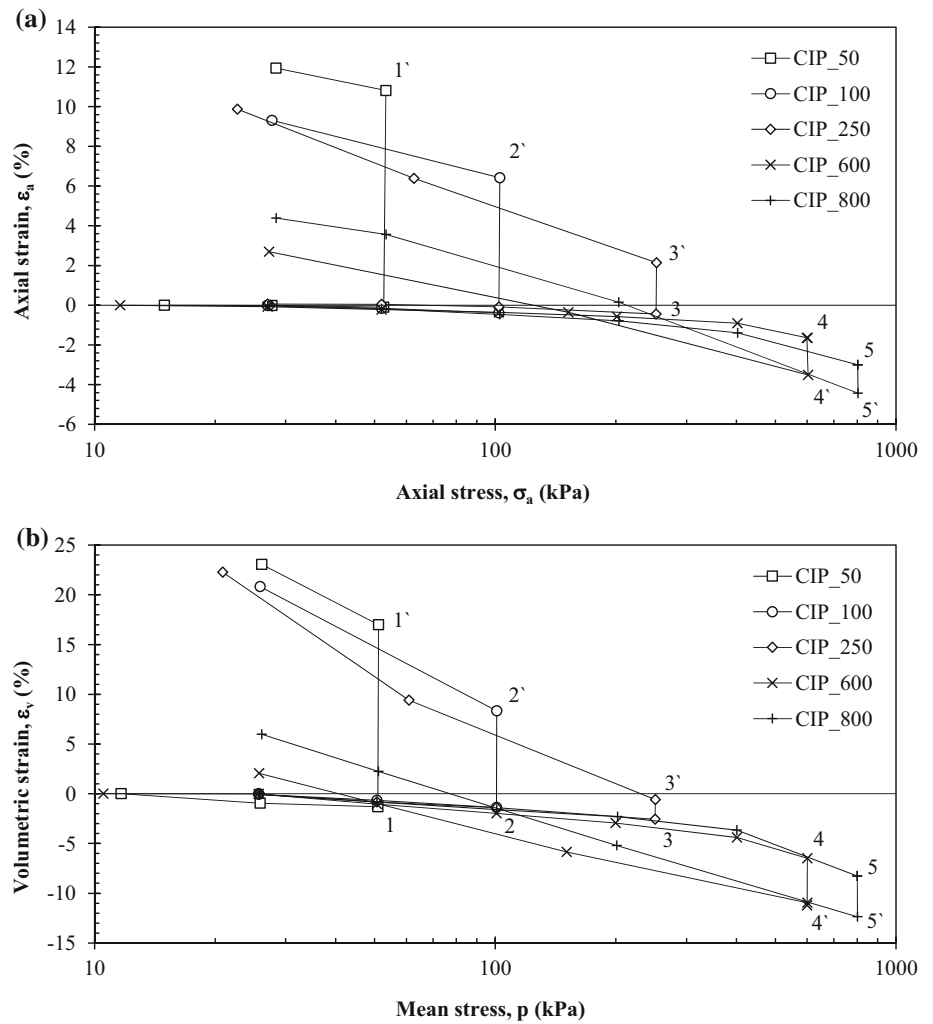
**Fig. 10** Axial strain versus axial stress for O_B samples
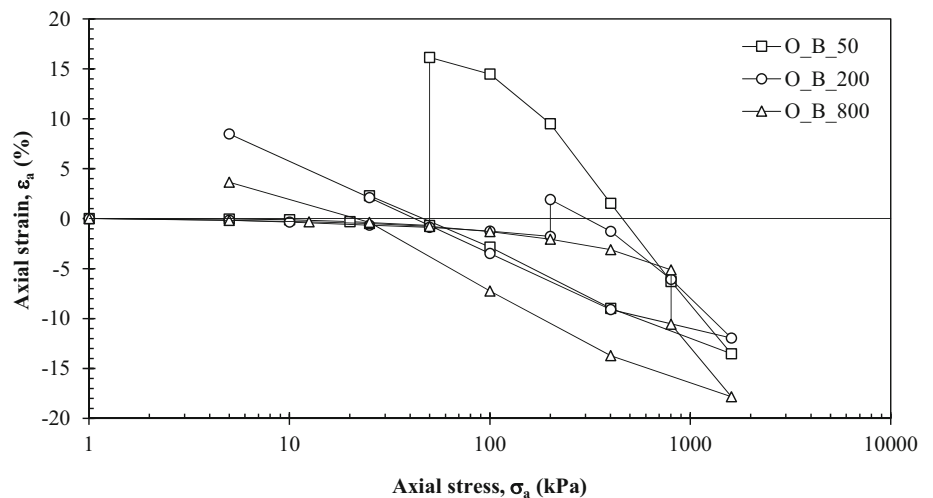
During inundation, the response-to-wetting behavior for CA specimens in σ_a–ε_a coordinates is represented as a horizontal line (e.g., line 1–1′ in Fig. 12a). This horizontal line denotes the magnitude of change in axial stress that take place under no axial strain condition (i.e., CA test). Considering p–ε_v representation, the response-to-wetting is delineated as an inclined line (e.g., line 1–1′ in Fig. 12b).

Fig. 11 Axial strain versus axial stress for the O_C method
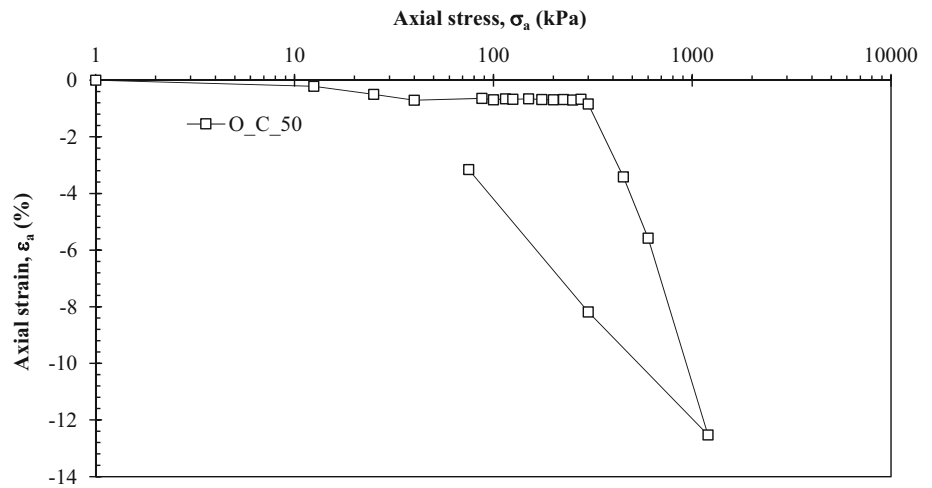
Fig. 12 Response-to-wetting curves for CA specimens
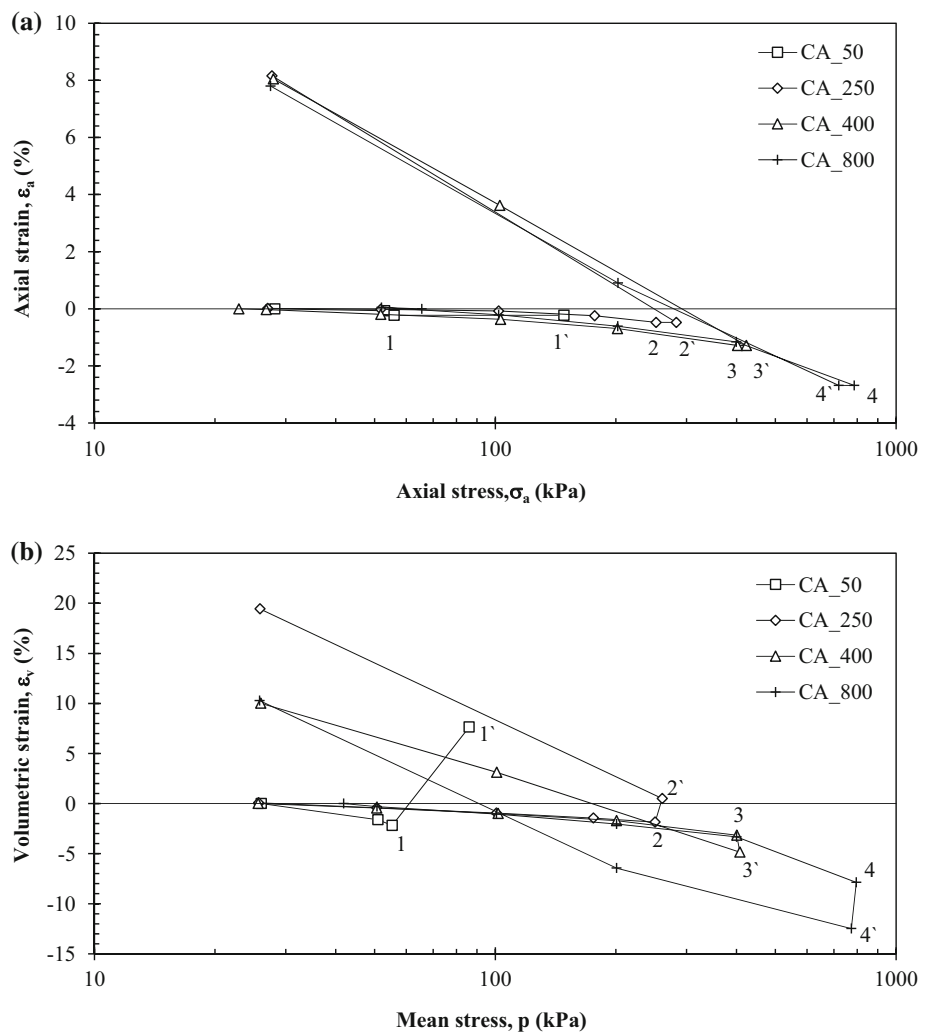
The response-to-wetting curves for CV specimens are illustrated in Fig. 13. Figure 13a shows the σ_a–ε_a relationship similar to that for CA specimens. For the p–ε_v representation, it is expected that the inundation stage be represented as a horizontal line indicating an increase in stresses with zero volume change. However, when examining Fig. 13b, it was observed that some volumetric strain was recorded. This is attributed to lateral strains (ε_L) developed

Fig. 13 Response-to-wetting for CV specimens
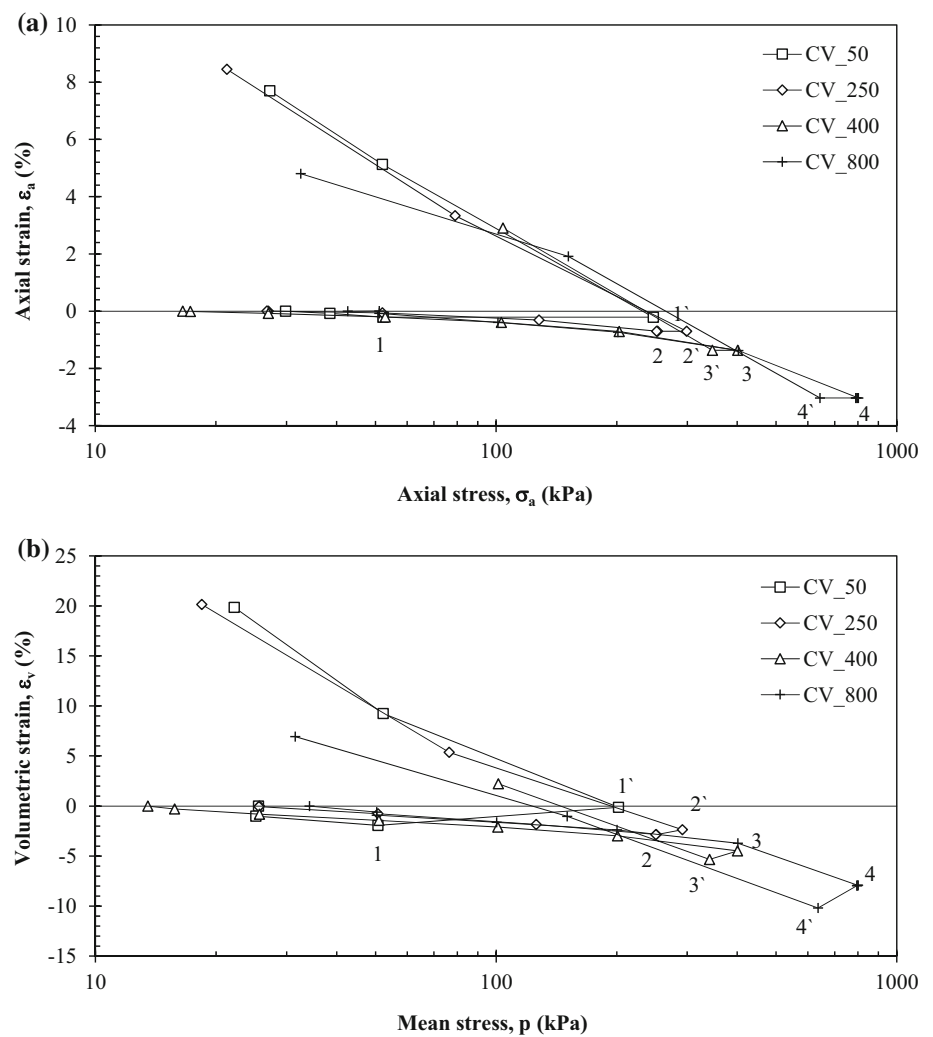
during inundation because of cell water compressibility imposing partial lateral restraint on the specimens. As stated earlier, the maximum error in lateral strain did not exceed 1.3 % (Table 1) which can be considered small.

Because of reduced specimen size considered in this study, it is important to assess the effect of end-platen friction on the quality of test results presented in Figs. 9, 12 and 13. For CV tests, the specimen was restrained in both lateral and axial direction. Hence, relative movement did not take place between the specimen and platen and end-platen friction is not relevant. In case of CIP and CA tests, radial strains in test specimens were permitted. Because of the axially restrained condition imposed during CA tests, the end-platen friction was of concern, especially when swelling was expected. In cases of CA specimens experiencing collapse, end-platen friction was considered to be negligible. A visual inspection of CA specimens that underwent swelling revealed that specimens showed small bulging. Based on this visual observation, end-platen friction was deemed to have a minor effect on test results.
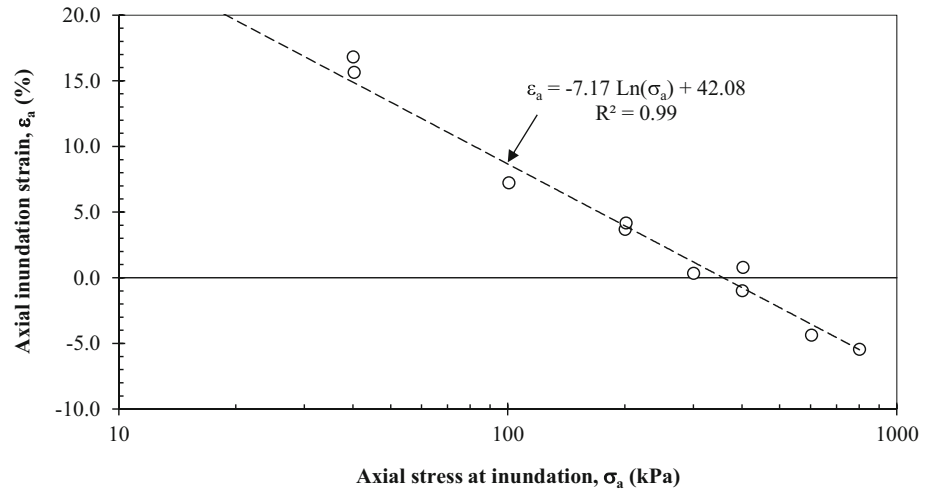
Inundation strains

In order to assess the influence of boundary and stress conditions on the volume change behavior of expansive clay under O_B, CIP and CA test conditions, relationships between inundation strain and logarithm stress upon inundation for each test series are plotted as shown in Figs. 14 through 17. Inundation strain is defined as the maximum component of strain (whether axial, lateral, or volumetric) attained due to wetting. Figure 14 shows a linear relationship between axial inundation strain and the logarithm of axial stress upon inundation for O_B specimens. Depending on axial stress upon inundation, specimens may experience swelling or collapse behavior. A similar trend to that observed in the swelling zone of Fig. 14 was reported by Grob (1972) and is known as Grob's law. The stress at which transition between swelling and collapse behavior occurs is considered the swelling pressure (defined by the intercept of the linear relationship with the horizontal axis). Similar conclusions can be

derived from Fig. 15 showing linear variation of different components of inundation strain for CIP specimens with the logarithm of the confining pressure upon inundation

(σ_c). From Fig. 15, it is observed that Grob's law (1972) is also valid for lateral and volumetric swelling strains. Combining Figs. 14 and 15 into Fig. 16 clearly revealed
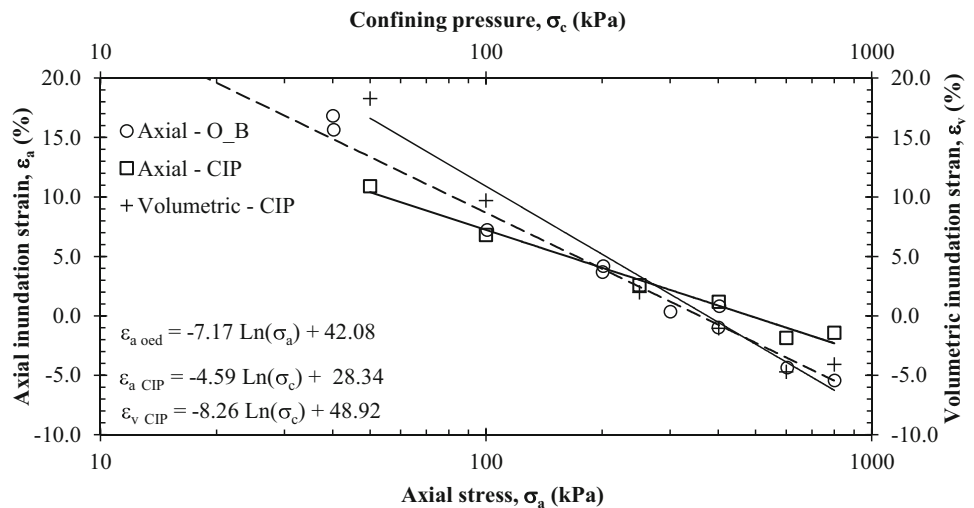
Fig. 14 Relation between axial inundation strain and axial stress upon inundation for O_B specimens

Fig. 15 Relations between inundation strains (volumetric, axial and radial) and confining pressure upon inundation for CIP specimens
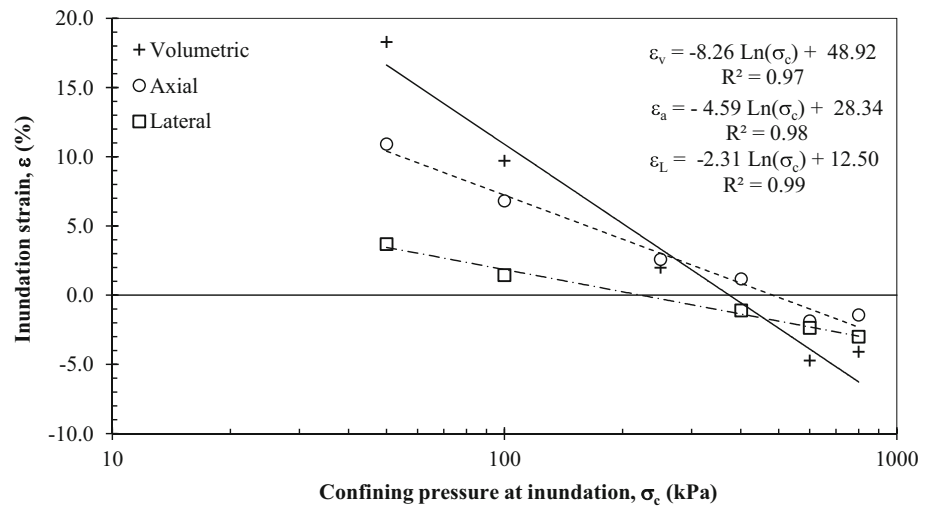
Fig. 16 Comparison between inundation strain and stress for O_B and CIP specimens

that the magnitude of axial inundation strain depends on test conditions. Specifically, the axial swell strain deduced from O_B tests was greater than that deduced from CIP. This is attributed to the higher level of lateral restraint imposed on O_B specimens than CIP specimens. However, the volumetric swelling pressure (i.e., applied mean stress corresponding to zero volumetric strain) deduced from CIP and O_B specimens are almost the same.

To investigate the effect of boundary conditions on the specimens' lateral strains, the lateral inundation strains for CIP and CA specimens were computed using the following equations:

$$\varepsilon_L = \frac{\varepsilon_v - \varepsilon_a}{2} \tag{1}$$

where ε_v, ε_a and ε_L are volumetric, axial and lateral strain, respectively.

The variations of lateral inundation strains with confining pressure upon inundation for CIP and CA specimens are illustrated in Fig. 17. From Fig. 17, the lateral inundation strain in case of CA is observed to be significantly higher than that of CIP due to axial restraint imposed on specimens causing most of the swelling energy to be directed towards a lateral direction.
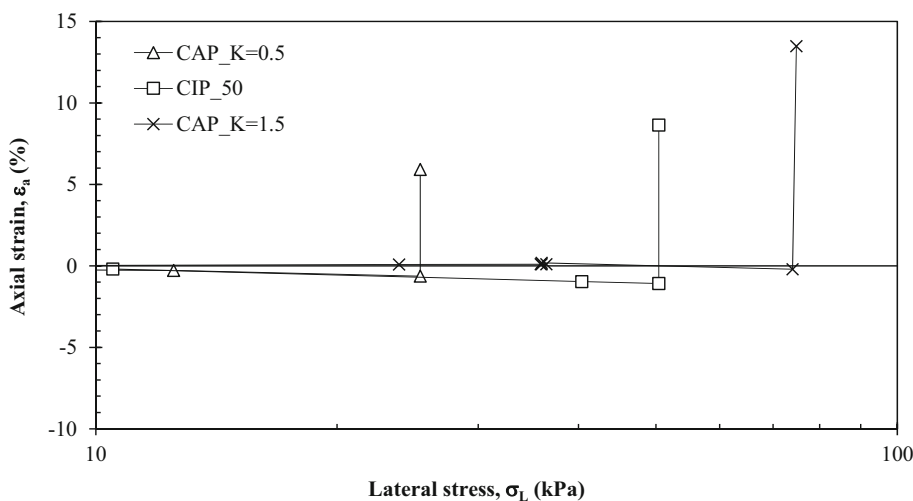
Effect of stress ratio on swell strain

The response-to-wetting curves for CAP specimens under different stress ratios (K) are illustrated in Fig. 18. From this figure, it can be inferred that as the stress ratio applied on specimens increases, the axial swelling strain increases. Combining data obtained from CIP (representing $K = 1.0$) and CAP tests, the variation of axial and volumetric swell strains with stress ratio was plotted, as shown in Fig. 19. From Fig. 19, it is observed that the stress ratio has a significant effect on the axial and volumetric swell strains, with these strains increasing exponentially with stress ratio.
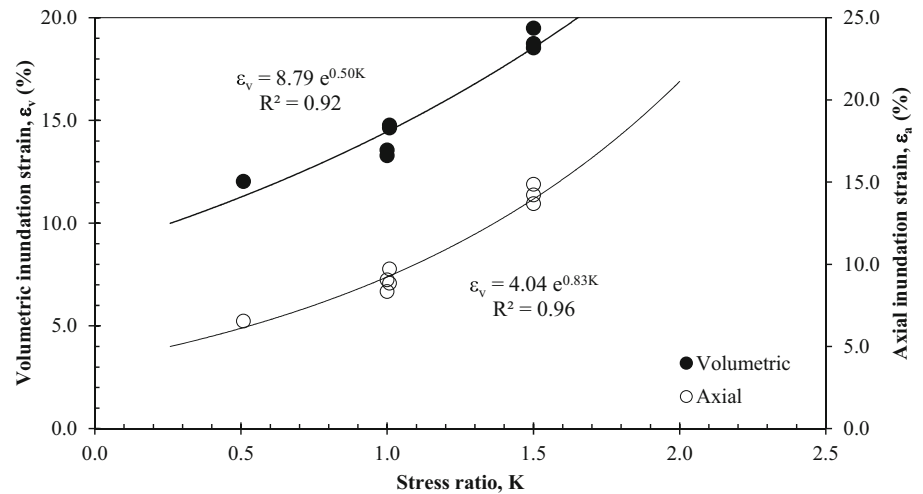

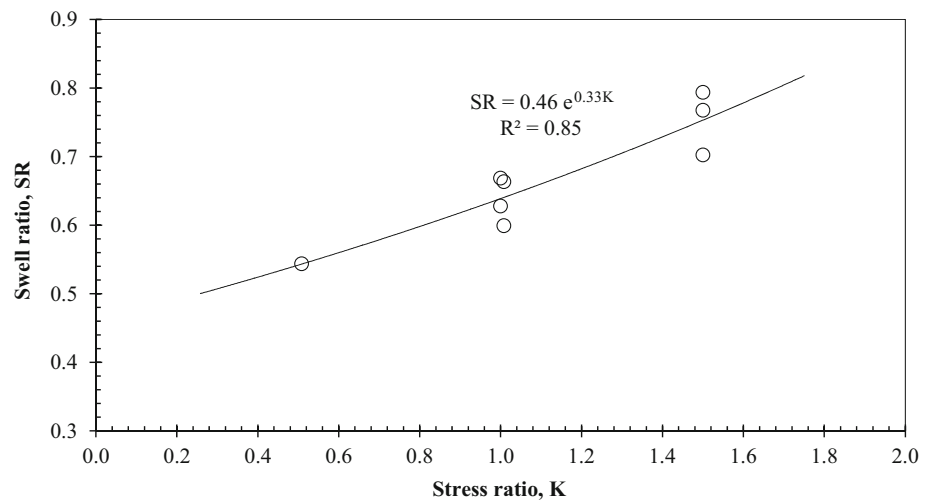**Fig. 17** Lateral inundation strains for CIP and CA specimens
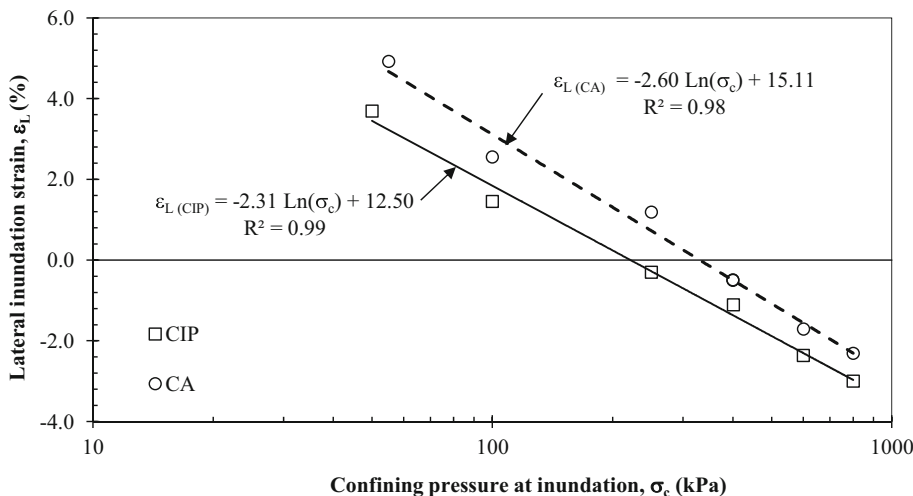
Fig. 18 Effect of stress ratio on response-to-wetting curves at $\sigma_L = 50$ kPa

Fig. 19 Effect of stress ratio on axial and volumetric swell strain for CAP specimens

Fig. 20 Relationship between swell ratio and stress ratio

The data in Fig. 19 was also combined to provide a relationship of swell ratio (SR)—defined as the ratio of the axial to the volumetric swell strain obtained from triaxial tests (i.e., CAP and CIP tests)—as a function of stress ratio, as shown in Fig. 20. Based on Fig. 20, the relative contribution of axial swell strain to volumetric strain ranged between 0.54 and 0.78 which is higher than that reported in the technical literature.

Because conventional oedometers are routinely used to evaluate the swelling potential of expansive soils and due to discrepancies between oedometer measurements and in situ axial swell strain measurements, a heave reduction factor was proposed to estimate axial swell strain anticipated under given boundary and stress conditions. For the soil considered in this study, a heave reduction factor, R_f, is defined as the ratio of the axial swell strain obtained from triaxial tests (i.e., CIP_50/Fig. 9 and CAP/Fig. 18) to that obtained from the oedometer test (i.e., O_B_50) under a constant axial stress of 50 kPa. A plot for the variation of R_f with stress ratio is

shown in Fig. 21. This figure revealed that R_f increased exponentially with stress ratio and ranged between 0.25 and 0.85. A plausible explanation for this trend is as the stress ratio, K (i.e., lateral stress, σ_L) increases, the degree of lateral restraint in a triaxial specimen increases, causing the swelling potential to be favorably directed in the vertical direction. This figure can aid in estimating the in situ axial swell strain provided that the oedometric axial swell and in situ stress ratio are known.

Stress state due to inundation

As stated earlier, CA tests simulate specimens that are restrained in axial conditions, while CV tests simulate specimens that are confined in both axial and lateral directions. The restraint imposed on the specimen will inhibit the development of strain and cause changes in specimen stresses. This section describes the stresses evolved during inundation of CA and CV specimens.

Fig. 21 Heave reduction factor versus stress ratio

$$R_f = 0.24\, e^{0.83K}$$
$$R^2 = 0.96$$
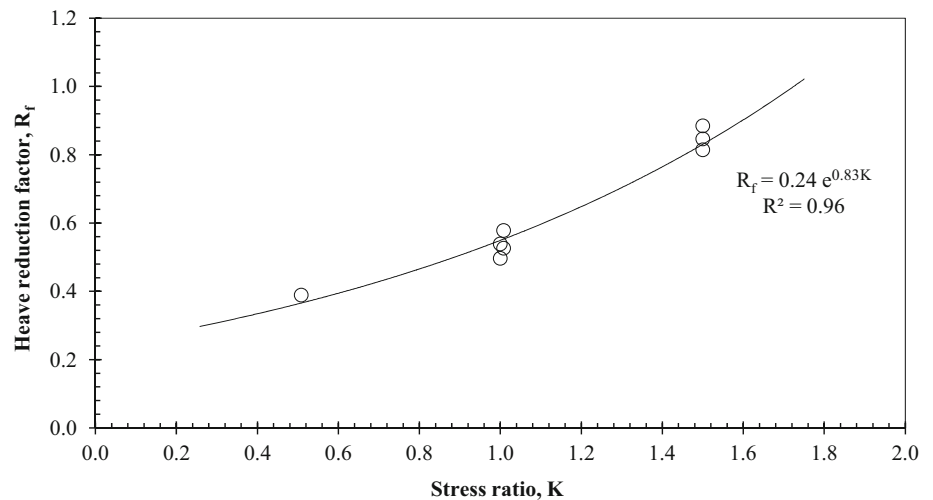
Fig. 22 Deviator stress development with time during CA specimens' inundation
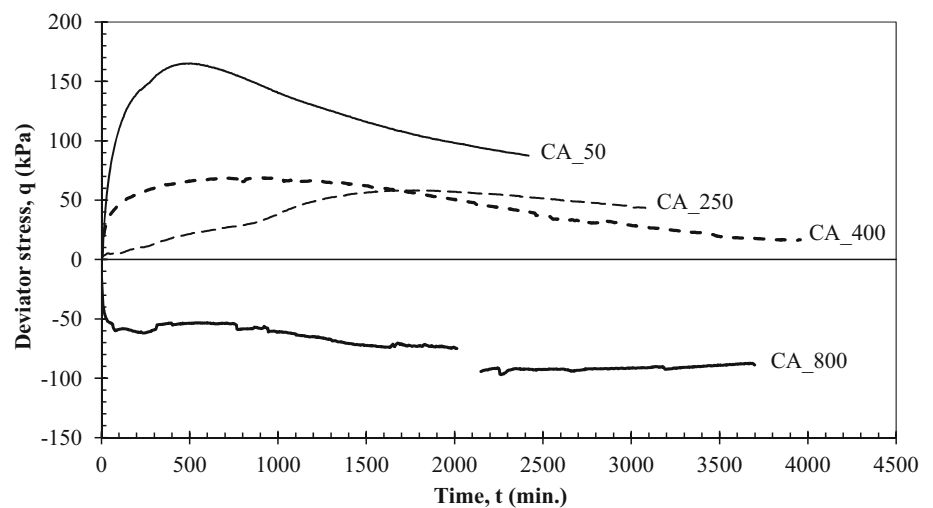
Constant axial (CA) deformation tests

Figure 22 shows the evolution of deviator stress ($q = \sigma_a - \sigma_L$) as a function of time under selected confining pressures upon inundation (σ_c). The trends for q versus time curves were observed to depend on σ_c. Under low confining pressure upon inundation, the gradual increase in deviator stress with time showed a "strain softening" behavior characterized by a definite peak value followed by reduction to a residual value. This phenomenon postulates that CA specimens experienced shear loss at the aggregate level due to an increase in deviator stress. This is evident by the reduction in K with time as presented in Fig. 23. As the confining pressure upon inundation increased (Fig. 22), the peak deviator stress decreased, reaching a negative value (extension stress) due to the specimen's tendency to collapse (at confining pressure upon inundation greater than 400 kPa). The summary of data illustrated in Fig. 24 shows that the confining pressure upon inundation had a significant effect on the maximum deviator stress generated.

Constant volume (CV) tests

The change in mean stress (Δp) with time due to CV specimen inundation is depicted in Fig. 25. Similar to that observed for CA specimens, the change in mean stress with time was observed to be high under low confining pressures upon inundation. Further increase in confining pressure upon inundation (greater than 400 kPa) caused specimens to undergo collapse and the development of extension stresses (negative deviator stress). The effect of confining pressure upon inundation on the maximum deviator stress generated and lateral stress change is expressed as a linear trend, as shown in Fig. 26.

Stress paths during swell

For the full understanding of stresses imposed on specimens during swelling, the total stress paths followed by CA and CV specimens during swelling were plotted, as illustrated in Figs. 27 and 28, respectively. Both stress paths
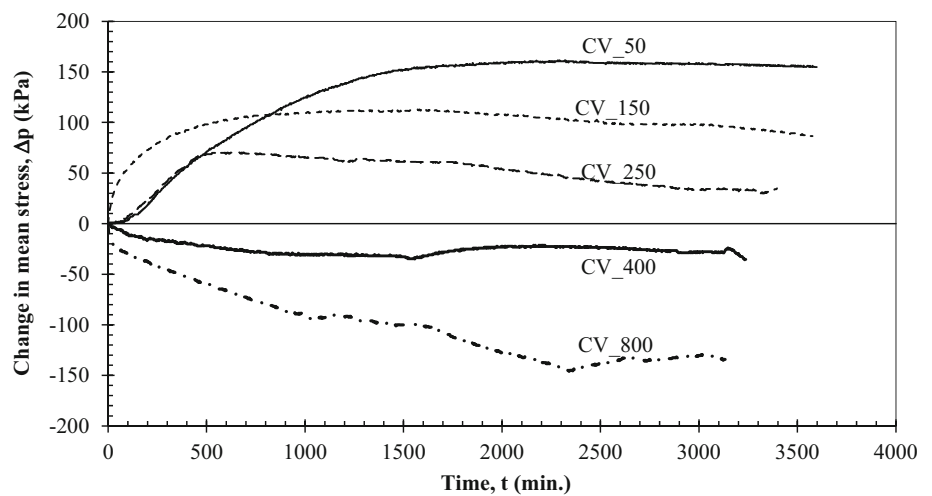
Fig. 23 Variation of stress ratio with time for CA tests
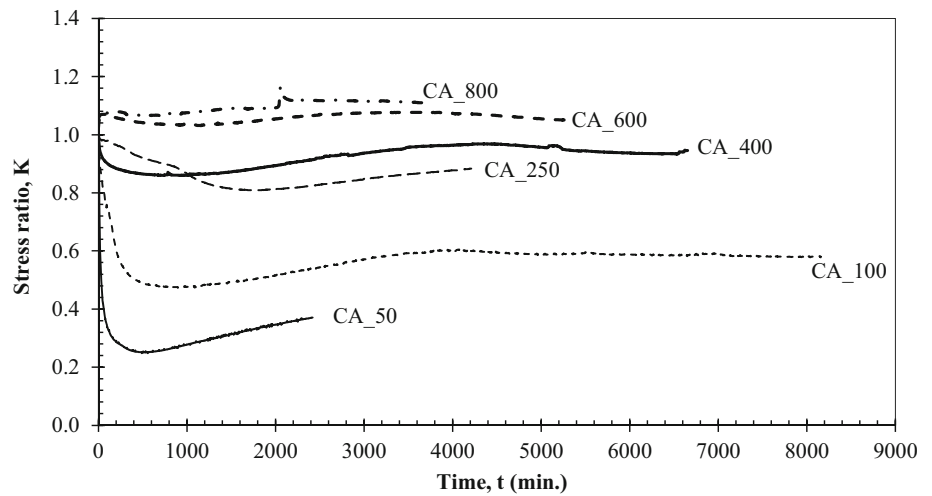
Fig. 24 Relationship between deviator stress (peak and residual) and confining pressure upon inundation for CA tests
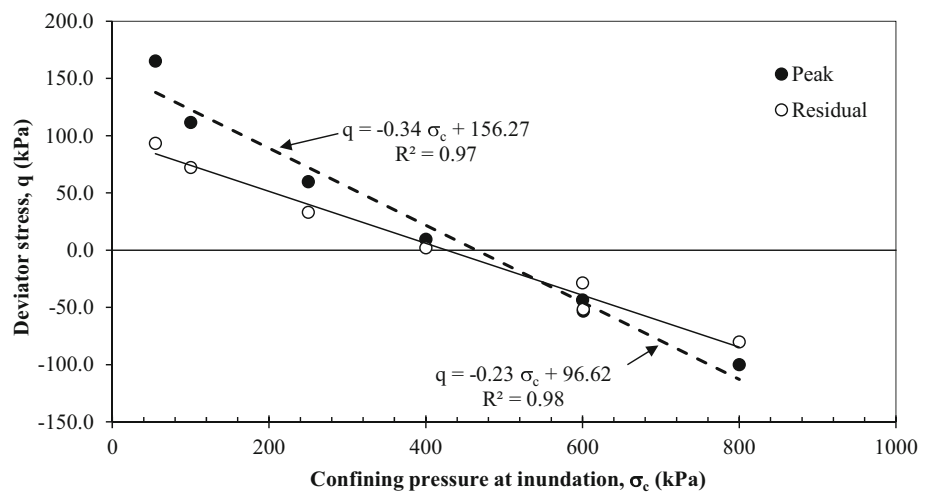
Fig. 25 Change in mean stress with time during inundation of CV specimens


showed increasing deviator stress trends reaching a peak value followed by a decrease to a residual stress value. Under CA cond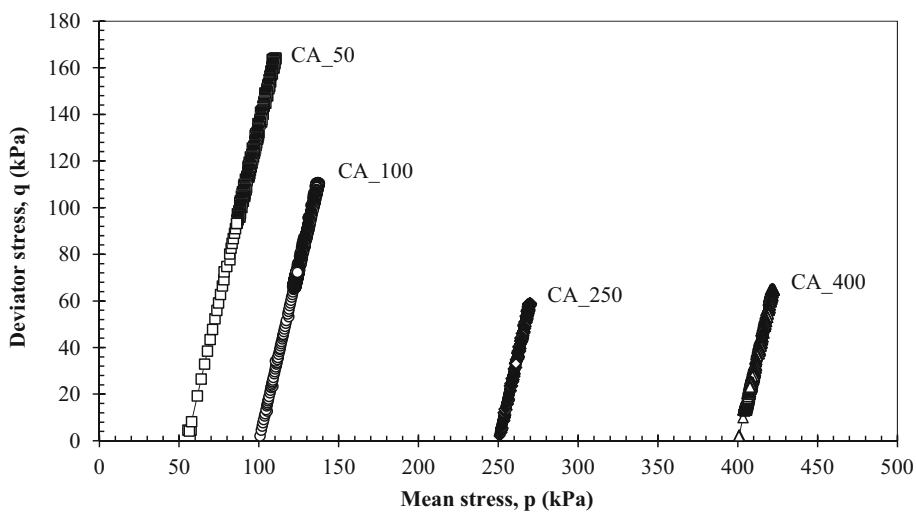itions, the increase and decrease in stress paths followed a single path as lateral stress acting on the specimen remained unchanged. Under CV conditions, the lateral stresses increased during swelling due to restraint
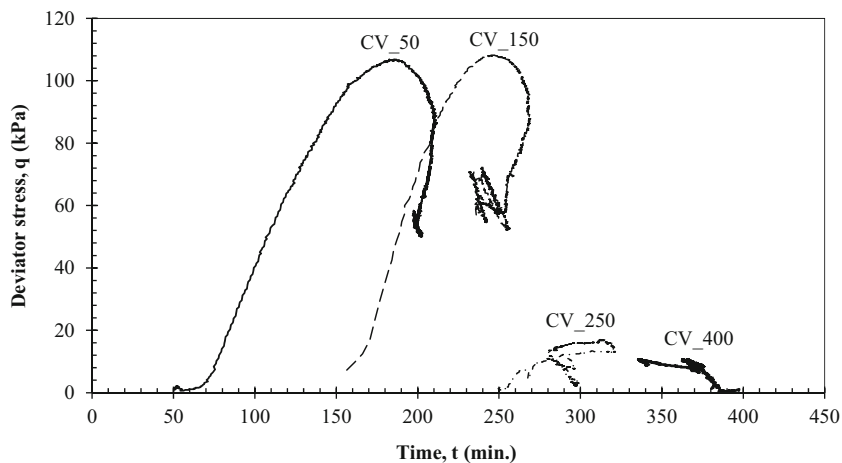
Fig. 26 Relationship between stress changes during inundation and confining pressure upon inundation during the CV inundation stage

$$\Delta\sigma_a = -0.59\ \sigma_c + 242.46$$
$$R^2 = 0.94$$

$$\Delta\sigma_c = -0.49\ \sigma_c + 160.10$$
$$R^2 = 0.94$$
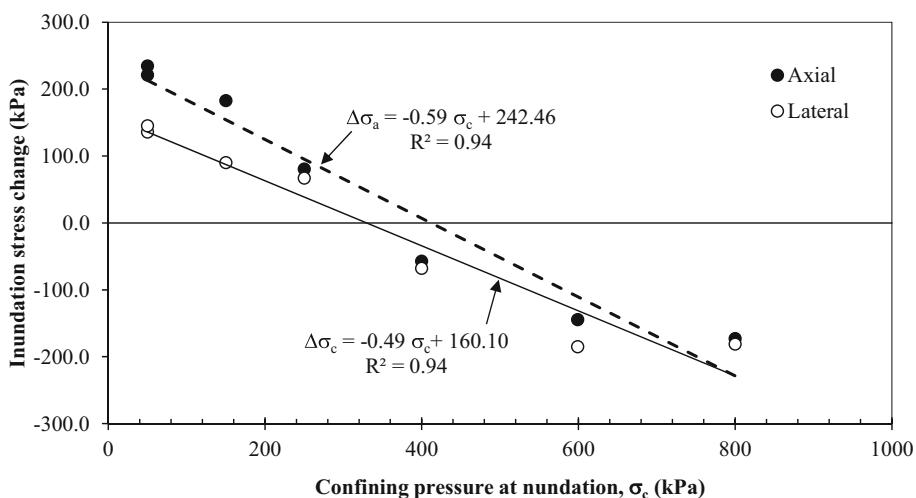
Fig. 27 Total stress path for CA specimens during swelling

Fig. 28 Total stress path for CV specimens during swelling

imposed, and this is depicted by the increase and decrease in stress paths following different paths. Furthermore, the inclination of the increasing stress path (Fig. 27 and 28) indicates that the rate of increase in deviator stress is greater than the rate of increase in lateral stress due to anisotropy of the specimen.

Conclusions

This study experimentally demonstrated the influence of the stress and deformation boundary conditions on the multi-directional (i.e., axial and lateral) stress and strain behavior of compacted, highly expansive clay. Response-to-wetting curves were used as a simple representation to delineate the state of strains and stress in specimens before and after wetting. Different trends for response-to-wetting curves emerged depending on boundary conditions applied.

With respect to volume change behavior, it was observed that the axial swell strains for CIP and CAP specimens were less than that observed by oedometer specimens because of the full lateral restraint imposed on oedometer specimens during inundation. Furthermore, the stress ratio ($K = \sigma_L/\sigma_a$) was observed to have a significant effect on axial and volumetric strain that increase exponentially with an increase in stress ratio. To quantify the effect of stress ratio (K; i.e., lateral restraint) on the axial swelling strain, the authors adopted the heave reduction factor, R_f, which represents the ratio between the axial swell strain obtained from triaxial testing and that obtained from oedometer testing. By definition, R_f will vary with stress ratio applied on a triaxial specimen. An increase in stress ratio (K) signifies an increase in lateral restraint, resulting in an increase in axial swell strain, as shown in Fig. 21. For the range of stress ratios considered in this study, the R_f value was observed to range between 0.25 and 0.85. This factor can be used to estimate the axial swell in the field based on oedometer axial swell strain and provided that the stress ratio is known.

Plots for the variation of deviator stress with time and total stress paths plots for CA and CV specimens identified a strain-softening behavior characterized by a peak and residual stress values. This suggests that specimens underwent shear loss at the aggregate level due to specimen restraint to swelling.

In conclusion, this study highlights the importance of evaluating the behavior of expansive soils under realistic stress and deformation boundary conditions for the proper estimation of state of strains and stresses in the specimens.

References

Abduljauwad SN (1994) Swelling behavior of calcareous clays from the Eastern Province of Saudi Arabia. Q J Eng Geol 27:333–351

Abduljuawad SN, Hameed RA, Al-Sulaimani GJ, Basunbal IA, Safar MM (1992) Expansive soils in eastern province of Saudi Arabia. In: Proceedings of 7th International Conference on Expansive Soils, Dallas, TX, Vol. 1:426–431

Al-Sayari SJ, Zotl JG (1978) Quaternary period in Saudi Arabia. Springer-Verlag, Wien

Al-Shamrani MA, Al-Mhaidib AI (1995) Multi-dimensional swell behaviour of expansive shales. In: Proceedings 11th African Regional Conference on Soil Mechanics and Foundation Engineering, XI ARCSMFE, Cairo, Egypt:161–174

Al-Shamrani MA, Al-Mhaidib AI (1999) Prediction of potential vertical swell of expansive soils using a triaxial stress path cell. Q J Eng Geol 32:45–54. doi:10.1144/GSL.QJEG.1999.032.P1.03

Al-Shamrani MA, Dhowian AW (2003) Experimental study of lateral restraint effects on the potential heave of expansive soils. Eng Geol 69(1–2):63–81. doi:10.1016/S0013-7952(02)00248-X

Al-Shayea N (2001) The combined effect of clay and moisture content on the behavior of remolded unsaturated soils. Eng Geol 62:319–342. doi:10.1016/S0013-7952(01)00032-1

ASTM D4546 (1996) Standard test methods for one-dimensional swell or settlement potential of cohesive soils. Annual Book of ASTM Standards, Section 4, vol. 04.08, Soil and Rock; Building Stones, West Conshohocken, PA

ASTM D698 (2000) Standard test methods for laboratory compaction characteristics of soil using standard effort. Annual Book of ASTM Standards, Section 4, vol. 04.08, Soil and Rock; Building Stones, ASTM, PA

ASTM D4767 (2011) Standard Test Methods for consolidated undrained triaxial compression test for cohesive soils. Annual Book of ASTM Standards, Section 4, vol. 04.08, Soil and Rock; Building Stones, West Conshohocken, PA

Azam S (2003) Influence of mineralogy on swelling and consolidation of soils in eastern Saudi Arabia. Can Geotech J 40:964–975. doi:10.1139/T03-047

Azam S, Al-Shayea NA (1999) Clayey behavior of calcareous soils. In: Proceedings, 2nd International Conference on Engineering for Calcareous Sediments, Bahrain. 1: 199–208

Azam S, Abduljauwad SN, Al-Shayea NA, Al-Amoudi OSB (1998) Expansive characteristics of gypsiferous/anhydritic formations. Eng Geol 51:89–107. doi:10.1016/S0013-7952(98)00044-1

Chen FH (1975) Foundations on expansive soils. Developments in Geotechnical Engineering, 12. Elsevier Scientific Publishing Co., Netherlands

Chen R, Ng CWW (2005) Wetting and anisotropic consolidation behavior of an expansive clay. In: Proceedings of the International Symposium on Advanced Experimental Unsaturated Soil Mechanics. Taylor and Francis Group, UK, pp 157–162

Dafalla M, Shamrani M (2011) Road damage due to expansive soils. Survey of the phenomenon and measures for improvement. design, construction, rehabilitation, and maintenance of bridges, ASCE, GSP 219, Hunan, China, June 9–11: 73–80. doi:10.1061/47630(409)10

Dafalla MA, Shamrani MA (2012) Expansive soil properties in a semi-arid region. Res J Environ Earth Sci 4(11):930–938

Dakshanamurthy V (1979) A stress-controlled study of swelling characteristics of compacted expansive clays. Geotech Test J 2(1):57–60. doi:10.1520/GTJ10588J

Dhowian AW (1990) Heave prediction techniques and design consideration on expansive soils. J King Saud Univ Eng Sci 2:355–377

El-Naggar Z (1988) Foundation problems in sabkha deposits. Short course on foundation engineering for practicing engineers. CE Department, KFUPM, Dhahran, pp SD1–SD54

El-Sayed ST, Rabbaa SA (1986) Factors affecting behaviour of expansive soils in the laboratory and field—a review. Geotech Eng 17(1):89–107

Erol AO, Dhowian AW, Youssef A (1987) Assessment of oedometer methods for heave prediction. Proc 6th Int Conf Expans Soils New Delhi India 1:99–103

Gizienski SF, Lee LJ (1965) Comparison of laboratory swell tests to small scale field tests. Engineering Effects of Moisture Changes in Soils, Concluding Proceedings. International Research Engineering Conference on Expansive Clay Soils. Texas A&M Press, College Station, TX, pp 108–119

Grob H (1972) Schwelldruck im Belchentunnel Proc. Int. Symp. für Untertagebau, Luzern, pp 99–119

Houston S, Dye H, Zapata C, Walsh K, Houston W (2011) Study of expansive soils and residential foundations on expansive soils in Arizona. J Perform Constr Facil 25(1):31–44

Kassif G, Baker R (1969) Swell pressure by uni and triaxial techniques. In: Proceedings of the 7th International Conference on Soil Mechanics and Foundation Engineering. Mexico, 1: 215–218

Komornik A, David DA (1969) Prediction of swelling pressure of clays. J Soil Mech Found Eng Div ASCE 95:209–225

Konyuhov AI, Maleki B (2006) The Persian Gulf Basin: geological history, sedimentary formations, and petroleum potential. Lithol Miner Resour 41(4):344–361

Lui XF, Buzzi OP, Vaunat J (2014) Influence of stress-volume path on swelling behavior of an expansive clay. Unsaturated soils: research and applications, Khalili, Russell, Khoshghalb (eds) Sydney, Australia, July 2–4:931–937

Mitchell JK (1993) Fundamentals of soil behavior, 2nd edn. John Wiley & Sons, Inc., New York

Ng CW, Zhan LT, Cui YJ (2002) A new simple system for measuring volume changes in unsaturated soils. Can Geotech J 39(2):757–764. doi:10.1139/T02-015

Ofer Z, Blight GE, Komornik A (1983) An insitu swelling pressure test. In: Proceedings of the 7th Asian Regional Conference on Soil Mechanics and Foundation Engineering, Haifa: 64–70

Rabbaa SA (1975) Factors affecting engineering properties of expansive soils. M.Sc. Thesis, Al-Azhar University, Cairo, Egypt

Radevsky R (2001) Expansive clay problems—how are they dealt with outside the US? Expansive Clay Soils and Vegetative Influence on Shallow Foundations: 172–191

Ranganatham BV, Satyanarayana B (1965) A rational method of predicting swelling potential for compacted expansive clays. In: Proceedings of the 6th International conference on Soil Mechanics and Foundation Engineering, Montreal 1 92–96

Saint-Marc P (1978) Arabian peninsula: Phanerozoic geology of the world ii: the Mesozoic. Elsevier Scientific Publishing Company, Amsterdam

Sing A (1967) Soil engineering in theory and practice. Asia Publishing House Co., Bombay

Slater DE (1983) Potential expansive soils in Arabian Peninsula. ASCE J Geotech Eng 109(5):744–746

Tang CS, Huang LM, Ye WM, Wang J, Liu YM (2013) Influence of boundary condition on the swelling behavior of GMZ01 buffer/backfilling material in HLW repository. Rock characterization, modelling and engineering design methods, 3rd ISRM SINOROCK Symposium Shanghai, China, 18–20 June Feng, Hudson, Tang (eds) Taylor Francis Group, London:199–204

Tisot JP, Aboushook M (1983) Triaxial study of swelling characteristics. In: Proceedings 7th Asian Regional Conference on Soil Mechanics and Foundation Engineering, Vol. 1:94– 97

Wray W, El-Garhy B, Youssef A (2005) Three-dimensional model for moisture and volume changes prediction in expansive soils. J Geotech Geoenviron Eng 131(3):311–324